

# OPTIMUM AEROELASTIC DESIGN OF A RESONANCE TYPE FLAPPING WING FOR MICRO AIR VEHICLES

Koji Isogai\*, Yuichi Kamisawa\* and Hiroyuki Sato\*  
\*Nippon Bunri University

**Keywords:** *Aeroelasticity, Flapping Wing, MAV, Optimization*

## Abstract

*Optimum aeroelastic design method of a resonance type flapping wing for Micro Air Vehicle is presented. The method employs Complex Method and a 3D Navier-Stokes code to determine the optimum structural and aerodynamic parameters of a two-degrees-of-freedom flapping wing system. The method is applied to the design of a dragonfly-type MAV, and it is shown, by numerical simulation, that the flapping wings thus designed can generate the enough lift which sustains its weight and the enough thrust which overcomes the body drag efficiently.*

## 1 Introduction

Recently, worldwide study on insect like Micro Aerial Vehicle has been intensified. One of the key technologies of such vehicles is the development of an efficient and light weight flapping wing. In order to generate lift and thrust efficiently, the wing should be oscillated in a coupled flapping (rotational oscillation around a flapping axis) and feathering motion (twisting motion around the span wise axis) for which the phase advance angle of the feathering motion ahead of the flapping motion is about 90 deg. There are two methods to give such motion to the wing. Those are the forced oscillation method and the resonance type oscillation method. The forced oscillation method gives a constant amplitude oscillation to the wing using the mechanism composed of cam and link, while the resonance type oscillation method utilizes the resonance phenomenon of the elastically supported wing by applying the external force oscillated at the natural frequency

of the system. The flapping wing system based on the former method becomes heavy due to the existence of cam and link. In addition to this, the fatal shortcoming of the former is that the amplitudes of the flapping and feathering motions cannot be changed depending on the various flight conditions. As shown by Kamisawa and Isogai[1] the optimum flapping wing motions of dragonfly changes largely depending on the flight condition. It is also clear that the additional aerodynamic forces, which are needed for stability and control of the vehicle, cannot be generated if the amplitudes of the flapping and feathering motions cannot be changed. On the other hand, the resonance type flapping wing system provides light weight device since it does not need cam and link mechanism. However, it has been believed that arbitrary control of the amplitudes and phase angle of the flapping wing motions has also been difficult. Recently, Isogai et al.[2] have proposed a new concept of two-degrees of freedom resonance type flapping wing which enables the arbitrary control of the flapping wing motions. In [2], Isogai et al. have shown the theoretical basis of the concept and demonstrated its feasibility by the numerical simulation using 3D Navier-Stokes code which takes into account the aeroelastic effects.

The analytical model of the two-degrees-of-freedom resonance type flapping wing system we have proposed is shown in Fig. 1. The wing which is assumed to be rigid is supported elastically for flapping and feathering motions, by the springs whose spring constants are  $K_\phi$  and  $K_\theta$ , respectively. In the figure  $\phi$  and  $\theta$  are flapping and feathering angular displacements, respectively.  $Q$  is the torque around the flapping axis, which is applied to excite the system. As

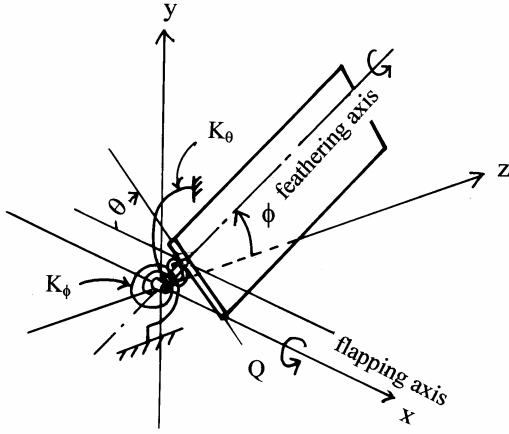


Fig. 1. Sketch of two-degrees-of-freedom resonance type flapping wing.

shown in [2], it is easy to derive the equations of motion of the system and to obtain the analytical solution of them when we neglect the effects of the aerodynamic forces by assuming that the stiffness of the springs are large enough for neglecting the aerodynamic forces. By coupling the analytical solution with an optimization algorithm, we have determined the structural parameters of the wing (mass and moment of inertia distributions), strengths of springs (or uncoupled natural frequencies of the system) and the amounts of torque and damping as the nondimensional quantities, that realize the wing motion specified by the designer (for example, the wing motion at hovering condition). As the next step, they have demonstrated [2] that the arbitrary wing motions (amplitudes of flapping and feathering motions) can be realized only by changing the amount of damping without changing the structural parameters and the amount of the applied torque, that are determined in the first step. The results obtained in [2] could be applied to the insect-type flapping wing whose springs are sufficiently stiff compared with aerodynamic stiffness. As the application of this concept, they have applied it to the dragonfly type flying robot (the full span 20 cm; mass 20 g; flapping frequency 34 Hz; we call this model as NBU model), which is under development at Nippon Bunri University. In order to evaluate the effect

of the aerodynamic force, which was neglected in the optimum design, they conducted the numerical simulation using the 3D Navier-Stokes code [3], [4]. As the results of the numerical simulation, it became clear that the phase difference between the flapping and feathering motions show about 50deg deviation from the ideal 90deg due to the aerodynamic effects. As a results of this, the flapping wing motions obtained are not necessarily efficient. In order to improve this point, the optimum aeroelastic design which couples the equations of motion of the resonance type flapping wing including the aerodynamic effect with the optimization algorithm might be effective to obtain the more efficient flapping wing. In this paper, we will present such an optimum aeroelastic design of the two-degrees-of-freedom resonance type flapping wing system using the 3D Navier-Stokes code as the aerodynamic tool.

## 2 Numerical Simulation of Two-Degrees-Of-Freedom Resonance Type Flapping Wing

For the numerical simulation of the present two-degrees-of-freedom (2DOF) resonance type flapping wing, we employ modal approach which utilizes the natural vibration modes of the present 2DOF flapping wing system. That is, the displacement of the wing in y direction can be expressed as

$$y(x, z, t) = \sum_{i=1}^2 \phi_i(x, z) q_i(t) \quad (1)$$

where  $\phi_i$  is the i-th natural vibration mode and its analytical solution can easily be obtained, and where  $q_i$  is the generalized coordinate. By employing the Lagrange's equations of motion, we obtain the ordinary differential equations for  $q_i$ , which gives the aeroelastic response of the system as follows:

$$M_i \ddot{q}_i + (\omega_i^2 / \omega) g_i M_i \dot{q}_i + \omega_i^2 M_i q_i = \iint_S \Delta p(x, z, t) \phi_i(x, z) dx dz + Q_0 \sin \omega t \quad \text{for } i=1, 2 \quad (2)$$

where  $Q_0$  and  $\omega$  are amplitude and circular frequency of the applied torque, and where  $M_i$  is the generalized mass of the semispan wing and is given by

$$M_i = I_\phi + 2S_\theta K_i + I_\theta K_i^2 \quad \text{for } i=1, 2 \quad (3)$$

where  $I_\phi$ ,  $S_\theta$ ,  $I_\theta$ ,  $K_i$  are defined by the following equations:

$$I_\phi = \int_{z_r}^{z_t} z^2 \left\{ \int_{chord} m(x, z) dx \right\} dz \quad (4)$$

$$S_\theta = \int_{z_r}^{z_t} z \left\{ \int_{chord} m(x, z) x dx \right\} dz \quad (5)$$

$$I_\theta = \int_{z_r}^{z_t} \left\{ \int_{chord} m(x, z) x^2 dx \right\} dz \quad (6)$$

$$K_i = (I_\phi / S_\theta) (-1 + (\omega_\phi / \omega_i)^2) \quad \text{for } i=1, 2 \quad (7)$$

where  $m(x, z)$  is the mass per unit area of the wing, and where  $z_r$  and  $z_t$  are  $z$ -coordinates of the root and tip stations of the wing, respectively. In Eqs. (2),  $\omega_i$  is the natural circular frequency of the system, the analytical solutions of which can easily be obtained as the functions of the uncoupled natural circular frequencies  $\omega_\phi$ ,  $\omega_\theta$  and the inertial parameters  $I_\phi$ ,  $I_\theta$  and  $S_\theta$ . The first terms of the right hand sides of Eqs. (2) are the generalized aerodynamic forces, and  $\Delta p(x, z, t)$  is the aerodynamic loading which is evaluated using the 3D Navier-Stokes code [3].  $g_i$  in Eq. (2) is the damping coefficient. In order to compute the aeroelastic response of the wing, Eq. (2) and the NS equations are solved at each time step using the finite difference technique. For the computation of the aeroelastic response of the flapping wings of the dragonfly type flying robot, which has two pair of wings, Eq. (2) can be applied to both the fore- and hind-wings, except that the second term of the right-hand side should be replaced by  $Q_0 \sin(\omega t + \Psi)$  for the hind-wing, where  $\Psi$  is the phase advance angle of the applied torque of the hind-wing ahead of the fore-wing.

## 2.2 Optimum Design of Two-Degrees-Of-Freedom Resonance Type Flapping Wings of Dragonfly-Type Robot

In order to determine the structural and aerodynamic parameters of the resonance type flapping wings of a dragonfly type flying robot, we have developed an optimization code by coupling the numerical simulation code described in the previous section and the optimization algorithm. The code is applied to the design of the dragonfly type robot which is under development at Nippon Bunri University (NBU). The sketch of the NBU model and the wing planform are shown in Figs. 2 and 3, respectively. The weight of the robot is 20gf.

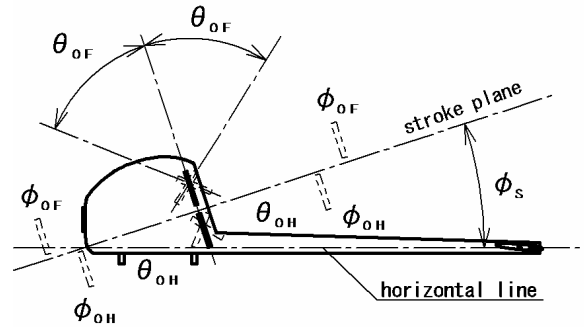


Fig. 2. Dragonfly type MAV.

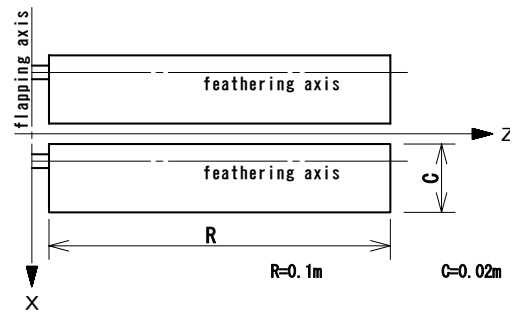


Fig. 3. Planforms of fore- and hind-wings.

In Fig. 2,  $\phi_s$  is the stroke-plane angle, and the suffixes F and H mean fore- and hind-wings, respectively. (It should be noted that  $y$ -axis shown in Fig. 1 coincides with the stroke-plane

shown in Fig. 2) As seen in Fig. 3, the robot has four rectangular wings of the same size. If we assume that the right and left wings flap symmetrically around the body axis ( $x$ -axis), it can easily be identified that the wing motions of the four resonance type flapping wings of the robot are governed by the following 18 dimensionless aerodynamic and structural parameters: that are

$$\begin{aligned} & k, \phi_s, \psi, S_{\theta f}/I_{\phi f}, I_{\theta f}/I_{\phi f}, \omega_{\phi f}/\omega, \omega_{\theta f}/\omega, I_{\phi h}/I_{\phi f}, \\ & S_{\theta h}/I_{\phi f}, I_{\theta h}/I_{\phi f}, \omega_{\phi h}/\omega, \omega_{\theta h}/\omega, \\ & Q_{\theta f}/(I_{\phi f} \omega_{\phi f}^2), Q_{\theta h}/(I_{\phi f} \omega_{\phi f}^2), g_{f1}, g_{f2}, g_{h1}, g_{h2} \end{aligned} \quad (8)$$

where  $k$  is the reduced frequency defined by  $b_f \omega / V_f$  ( $b_f$  is the semichord of the fore-wing,  $\omega$  is the frequency of excitation;  $V_f$  is the reference velocity and is 11.8 m/s);  $\phi_s$  is the stroke plane angle;  $g_1$  and  $g_2$  are the damping coefficients for the first and second natural modes, respectively, and where the suffixes  $f$  and  $h$  mean the fore- and hind-wings, respectively. It also should be noted that the parameters  $I_{\phi f}$  and  $V_f$  can be given by the designer. In the present optimization study, these 18 dimensionless quantities are taken to be the design variables, and the following function  $F$  is taken to be the objective function which is to be minimized, namely,

$$F = C_{w1}(L_{\text{target}} - L)^2 + C_{w2}(T_{\text{target}} - T)^2 \quad (9)$$

where  $L_{\text{target}}$  and  $T_{\text{target}}$  are the target lift and thrust, respectively, while  $L$  and  $T$  are the time mean lift and thrust, respectively, obtained by solving the equations of motion coupled with the 3D Navier-Stokes code.  $C_{w1}$  and  $C_{w2}$  in Eq. (9) are the weighting constants.  $L_{\text{target}}$  and  $T_{\text{target}}$  are the quantities given by the designer depending on the flight condition.

As the optimization algorithm, we employed the Complex Method [5] which is one of the direct search methods without recourse to the derivatives. In the Complex Method, the optimization process proceeds by the use of flexible figures of  $K > N+1$  vertices in  $N$  dimensional design space, where  $N$  is the number of design variables ( $N = 18$  in the

present problem) and we have taken  $K = 21$  vertices. In Fig. 4, four vertices (the points A, B, C and R) are shown for illustration purposes. Each vertex corresponds to a specific aero-elastic response of the wing, which is specified by the 18 design variables in the present problem. The objective function and the constraint functions ( $g_{f1}$ ,  $g_{f2}$ ,  $g_{h1}$ ,  $g_{h2}$  in the present problem) at each vertex are evaluated

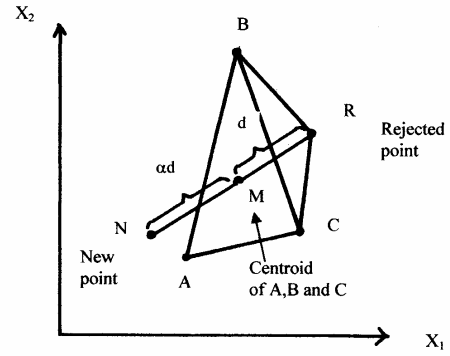


Fig. 4. Complex Method.

using the method described in the previous section. Then, the worst vertex (the vertex that gives the highest value of  $F$ : point R in Fig. 4) is found, and is rejected. A new point N is found such that the new point is located at a distance  $\alpha d$  from the centroid M of the vertices A, B and C in the opposite direction to R, where  $d$  is the distance between M and R, and where  $\alpha$  is a coefficient used to accelerate the convergence, usually taken as  $\alpha = 1.0-1.3$ . We call this process Rule 1. Next the objective function  $F$  and the constraint functions  $g_{f1}$ ,  $g_{f2}$ ,  $g_{h1}$ ,  $g_{h2}$  at the new point N are evaluated using the method described in the previous section. If the constraint function does not satisfy the specified value of the constraint, namely,  $g_{f1} > 0$ ,  $g_{f2} > 0$ ,  $g_{h1} > 0$ ,  $g_{h2} > 0$ , the point N is shifted toward the centroid M such that the distance between the new point N and M is half the previous distance. We call this process Rule 2. Rule 2 is repeated until the constraint is satisfied. Rule 1 and Rule 2 are repeated until the converged value of  $F$  is obtained. The 18 design variables that give a minimum  $F$  give the optimum aerodynamic and structural parameters of the robot. Further

details of the complex method are explained in [6].

Usually, it takes about 8 – 12 cycles of oscillation to obtain the converged periodic solution for one combination of 18 variables, consuming about 4 – 7 days of computation time on our computer (Intel Pentium 4 class PC). Therefore, we interrupted the computation at the iteration step of the optimization after 4 cycles of oscillations to save the computation time. (As shown later, we have obtained the relatively good results even if we took this measure.) Since the most important capability of the insect type flying robot is its hovering capability, we conducted the present optimization study of the NBU model for hovering condition. As pointed out previously, the designer can specify the values of  $I_{\phi f}$  and  $V_f$ , depending on the robot he wants to design. For the present NBU model, we gave the following values:

$$I_{\phi f}=2.27 \times 10^{-7} \text{ kgm}^2, \quad V_f=11.8 \text{ m/s}$$

As the target values of lift and thrust, we gave

$L_{\text{target}}=0.245 \text{ N}$  (1.25 times of the weight of the robot) and  $T_{\text{target}}=0$ .

In the Complex Method [5], the appropriate initial values of the design variables should be given before starting the iterative steps of the optimization. In the present study, we used the optimum design variables which were determined in [2], where the effects of the aerodynamic forces were neglected. As shown in Fig. 5, we have obtained the converged solution with  $F=O(10^{-4})$  after 65 iteration steps. The results thus obtained are as follows:

$$\begin{aligned} k &= 0.208, \phi_s = 1.6 \text{ deg}, \psi = 11.8 \text{ deg}, \\ S_{\theta f} &= 0.668 \times 10^{-7} \text{ kgm}^2, I_{\theta f} = 2.75 \times 10^{-7} \text{ kgm}^2, \\ \omega_{\phi f} &= 239.8 \text{ rad/s}, \omega_{\theta f} = 286.3 \text{ rad/s}, \\ I_{\phi h} &= 2.58 \times 10^{-7} \text{ kgm}^2, S_{\theta h} = 0.674 \times 10^{-7} \text{ kgm}^2, \\ I_{\theta h} &= 2.78 \times 10^{-7} \text{ kgm}^2, \\ \omega_{\phi h} &= 245.4 \text{ rad/s}, \omega_{\theta h} = 240.2 \text{ rad/s}, \\ Q_{\theta f} &= 0.0165 \text{ Nm}, Q_{\theta h} = 0.0204 \text{ Nm}, \\ g_{f1} &= 0.0888, g_{f2} = 0.0679, g_{h1} = 0.291, g_{h2} = 0.153, \end{aligned}$$

(10)

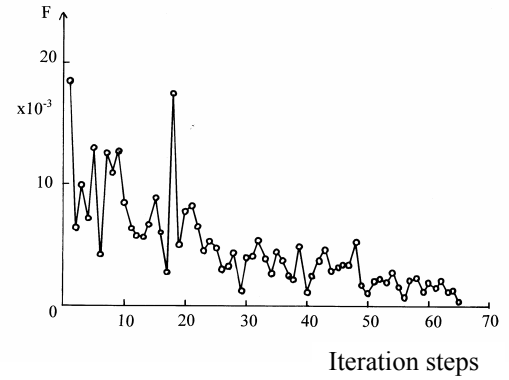


Fig. 5. Convergence history of iteration steps.

From the definition of  $k$ , the frequency of excitation is 244.9 rad/s (39.0 Hz). The coupled natural frequencies of the fore- and hind-wings are as follows:

$$\begin{aligned} \omega_{f1} &= 226.6 \text{ rad/s}, & \omega_{f2} &= 314.4 \text{ rad/s} \\ \omega_{h1} &= 217.0 \text{ rad/s}, & \omega_{h2} &= 280.6 \text{ rad/s} \end{aligned} \quad (11)$$

As described previously, the aeroelastic response computation at each iterative step was interrupted at 4 cycles of oscillation before the converged periodic solution was obtained. Therefore we have recalculated the aeroelastic responses of the wings for 12 cycles of oscillation using the optimum solution given by Eqs. (10). In Fig. 6, the aeroelastic response (the responses of the flapping and feathering displacements) of the fore- and hind-wings for 12 cycles of oscillation are shown. As seen in the figure, the periodic solution has been obtained after 4 – 8 cycles of oscillation. In Fig.7, the responses of the flapping and feathering displacements of the fore- and hind-wings at the 12th cycle of oscillation are shown. It is identified that the amplitudes of the flapping oscillations of fore- and hind-wings are 20 deg and 25 deg, respectively, and the amplitudes of the feathering oscillations of fore- and hind-wings are 31 deg and 28 deg, respectively, and that the phase differences between the flapping and feathering motions of

the fore- and hind-wings, that is important for the efficient lift and thrust generation, are 98 deg and 136 deg, respectively. The necessary power of 2.95 W is about 28% improvement over the optimum design [2] obtained by neglecting the effects of aerodynamic force. Fig. 8 shows the responses of lift and thrust at the 12th cycle of oscillation. The mean lift and thrust are 0.230 N (1.17 times of the weight of the robot) and 0.0 N, respectively. In Fig. 9, the flow patterns (iso-vorticity distribution) around fore- and hind-wings are shown.

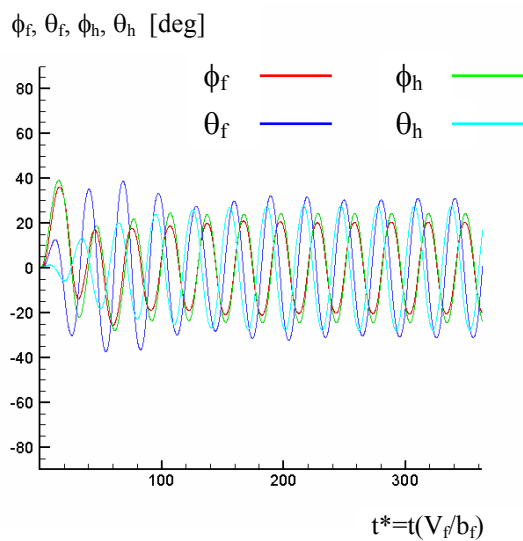


Fig. 6. Aeroelastic responses of the fore- and hind-wings for 12 cycles of oscillation.

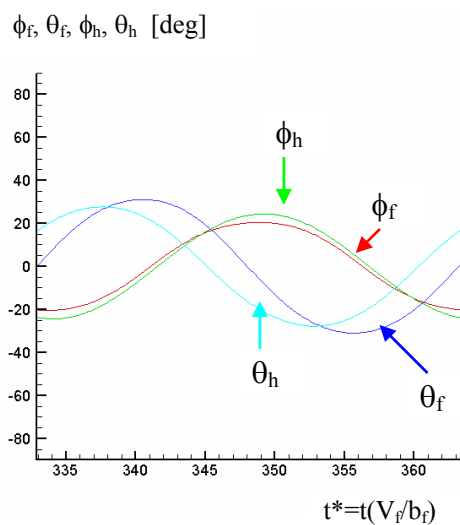


Fig. 7. Aeroelastic responses of fore- and hind-wings at 12th cycle of oscillation.

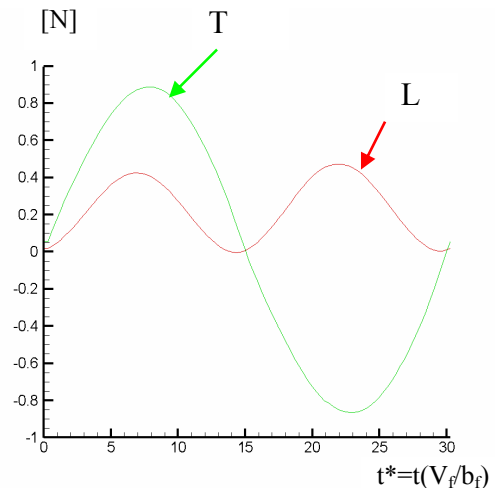
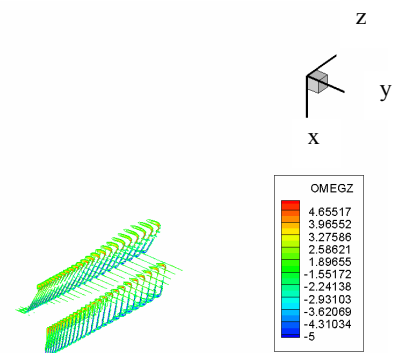


Fig. 8. Time histories of lift and thrust at 12th cycle of oscillation.



$$kt^* = 2\pi/3$$

Fig. 9. Flow patterns (iso-vorticity distribution) around a fore- and hind-wings for hovering condition.

As the next step, we have conducted the aeroelastic response computation for  $V=7\text{m/s}$ , where  $V$  is the advance velocity, to see whether the optimum design parameters determined for the hovering condition ( $V=0\text{ m/s}$ ) is still effective or not for other flight conditions. The computation for this case is performed using the same design parameters given by Eqs. (10) except that  $\phi_s$  and  $\Psi$  were replaced by 75 deg and 90 deg, respectively. Fig 10 shows the aeroelastic response of flapping and feathering

displacements of fore- and hind-wings at the 12th cycle of the oscillation.

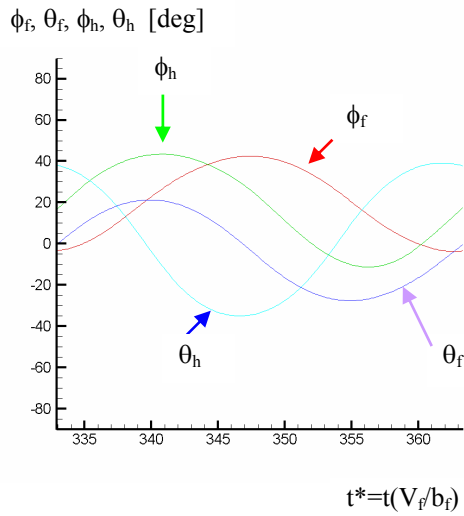


Fig. 10. Aeroelastic responses of fore- and hind-wings at 12th cycle of oscillation ( $V=7\text{m/s}$ ).

From the figure, it is identified that  $\phi_{of}=23$  deg,  $\phi_{mf}=20$  deg,  $\theta_{of}=24$  deg,  $\theta_{mf}=-4$ deg,  $\Delta\lambda_f=88$  deg,  $\phi_{oh}=28$  deg,  $\phi_{mh}=16$  deg,  $\theta_{oh}=37$  deg,  $\theta_{mh}=2$ deg and  $\Delta\lambda_h=113$  deg, where  $\phi_{mf}$  and  $\phi_{mh}$ ,  $\theta_{mf}$  and  $\theta_{mh}$  are the time mean values of the flapping and feathering displacements of the fore- and hind-wings, respectively. The phase differences ( $\Delta\lambda_f$ ,  $\Delta\lambda_h$ ) between the flapping and feathering oscillation are close to 90 deg both for the fore- and hind-wings. Fig. 11 shows the flow pattern (iso-vorticity distribution) around the fore- and hind-wings. Fig. 12 shows the time histories of lift and thrust. The time mean lift is 0.423 N which is 2.16 times of the weight of the robot and the time mean thrust is 0.115N which is grater than the estimated body drag of 0.086N. The necessary power predicted is 3.80 W for this case. From these results, we can conclude that the present resonance type flapping wings whose aerodynamic and structural parameters were determined for the hovering condition are still effective for  $V=7$  m/s.

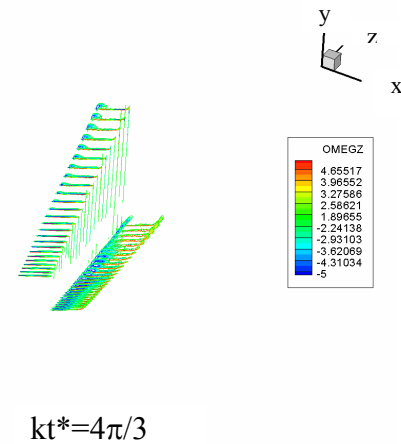


Fig. 11. Flow patterns (iso-vorticity distributions) around fore- and hind-wings

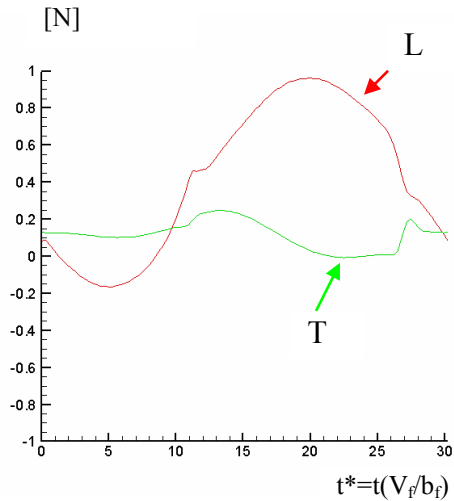


Fig. 12. Time histories of lift and thrust at 12th cycle of oscillation ( $V=7$  m/s).

### 5 Conclusion

Optimum aeroelastic design method of a resonance type flapping wing for Micro Air Vehicle is presented. The method employs Complex Method and a 3D Navier-Stokes code to determine the optimum structural and aerodynamic parameters of a two-degrees-of-freedom flapping wing system. The method is applied to the design of a dragonfly-type MAV, and it is shown, by numerical simulation, that

the flapping wings thus designed can generate the enough lift which sustains its weight and the enough thrust which overcomes the body drag efficiently.

### Acknowledgements

Authors acknowledge the support of Ministry of Education, Culture, Sports, Science and Technology of Japan under the High-Tech Research Center Promotion Program.

### References

- [1] Kamisawa, Y. and Isogai, K. Study on Optimum Flapping Motions of Dragonfly. ISABMEC2006, Ginowan, Okimawa, Paper No. P09, July 2006.
- [2] Isogai, K., Kamisawa, Y. and Sato, H., Resonance Type Flapping Wing for a Micro Air Vehicle. *AIAA Atmospheric Flight Mechanics Conference and Exhibit*, 20-23 August 2007, Hilton Head, South Carolina, AIAA 2007-6499, 2007.
- [3] Isogai, K., Fujishiro, S., Saito, T., Yamamoto, M., Yamasaki, M. and Matsubara, M., Unsteady Three-Dimensional Viscous Flow Simulation of a Dragonfly Hovering. *AIAA Journal*, Vol. 42, No. 10, pp. 2053 – 2058, 2004.
- [4] Yamamoto, M. and Isogai, K., Measurement of Unsteady Fluid Dynamic Forces for a Mechanical Dragonfly Model. *AIAA Journal*, Vol. 43, No. 12, pp. 2475 – 2480, 2005.
- [5] Box, M. J., A New Method of Constrained Optimization and Comparison with Other Methods. *Computer Journal*, Vol. 8, pp. 42 -52, 1965.
- [6] Beveridge, G. S. G., and Schecheter, R. S., *Optimization, Theory and Practice*. Chemical Engineering Series, McGraw Hill, New York, pp. 453-456, 1970.

### Copyright Statement

The authors confirm that they, and/or their company or institution, hold copyright on all of the original material included in their paper. They also confirm they have obtained permission, from the copyright holder of any third party material included in their paper, to publish it as part of their paper. The authors grant full permission for the publication and distribution of their paper as part of the ICAS2008 proceedings or as individual off-prints from the proceedings.